



2- β -Benzothiazolyl-6-iminopyridylmetal dichlorides and the catalytic behavior towards ethylene oligomerization and polymerization

Shengju Song^a, Rong Gao^a, Min Zhang^a, Yan Li^a, Fosong Wang^a, Wen-Hua Sun^{a,b,*}

^a Key Laboratory of Engineering Plastics and Beijing National Laboratory for Molecular Sciences, Institute of Chemistry, Chinese Academy of Sciences, Beijing 100190, China

^b State Key Laboratory for Oxo Synthesis and Selective Oxidation, Lanzhou Institute of Chemical Physics, Chinese Academy of Sciences, Lanzhou 730000, China

ARTICLE INFO

Article history:

Received 11 April 2011

Received in revised form 19 June 2011

Accepted 29 June 2011

Available online 5 July 2011

Keywords:

2- β -Benzothiazolyl-6-iminopyridine

Iron

Cobalt

Oligomerization

Polymerization

ABSTRACT

A series of 2-(2-benzothiazolyl)-6-(1-(arylimino)ethyl)pyridines and their metal (Fe or Co) complexes were prepared. All organic compounds were fully characterized by NMR, FT-IR spectra and elemental analysis, and all metal complexes were identified by FT-IR spectroscopic and elemental analysis. The molecular structures of representative metal complexes were confirmed by single-crystal X-ray diffraction and displayed the distorted trigonal bipyramid geometry. Upon activation with modified methylaluminoxane (MMAO), the iron pro-catalysts showed good catalytic activities up to the range of 10^7 g mol⁻¹(Fe) h⁻¹ in ethylene reactivity with the high selectivity for the vinyl-type products of both oligomers and polyethylene waxes; whereas the cobalt pro-catalysts showed moderate activities towards ethylene oligomerization. The correlations between metal complexes and their catalytic activities and products were investigated in detail under various reaction parameters and discussed.

© 2011 Elsevier B.V. All rights reserved.

1. Introduction

Since the 2,6-diiminopyridylmetal (Fe or Co) complexes were independently discovered as highly active pro-catalysts in ethylene polymerization by Bennett [1], Brookhart and co-workers [2] and Gibson and co-workers [3] in 1998, the derivatives of 2,6-diiminopyridylmetal complexes have been extensively investigated through fine-tuning substituents on 2,6-diiminopyridines [4–12]. Moreover, the metal (Fe or Co) complexes bearing non-symmetrical 2,6-diiminopyridines, which were prepared by the reaction of 2,6-diacetylpyridine with two different anilines (including an alkylamine sometime) instead of two identical anilines, were investigated with a view to modify their catalytic behavior [13–18]. In addition, new pro-catalysts performing interesting catalytic behavior have been achieved with employing newly designed ligands such as 2-ester-6-iminopyridines [19], 2-furan- or 2-thiophen-6-iminopyridines [20,21], 2-imino-1,10-phenanthrolines [22–26], 2-oxazoline/benzoxazole-1,10-phenanthrolines [27], 2-benzimidazolyl-1,10-phenanthrolines [28], *N*-(2-pyridylmethyl)-2-quinolin-8-amines [29], 2-quinoxalyl-6-iminopyridines [30], 2-benzimidazolyl-6-iminopyridines [31–33], and 2-benzoxazolyl-

6-imino-pyridines [34,35]. Several review articles have highlighted the progress of these research achievements [36–42].

Both pro-catalysts containing 2-benzimidazolyl- or 2-benzoxazolyl-substituted 6-iminopyridines, **A** [31–33] and **B** [34,35] in Scheme 1, were developed and showed competitive activities towards ethylene. 2-Thiophen-6-iminopyridylcobalt pro-catalysts had better activities than 2-furan-6-iminopyridylcobalt analogs [20,21], and 2-(2-benzoxazolyl)-1,10-phenanthrolylchromium pro-catalysts showed better activities than 2-(2-benzothiazolyl)-1,10-phenanthrolylchromium analogs [43]. As a consequent work, the pro-catalysts containing 2- β -benzothiazolyl-6-iminopyridines (**C** in Scheme 1) are necessarily investigated with the comparison of their analogs **A** and **B**. Herein the syntheses and characterization of metal (Fe or Co) complexes bearing 2-(2-benzothiazolyl)-6-iminopyridines are reported along with their catalytic behavior in ethylene oligomerization and polymerization.

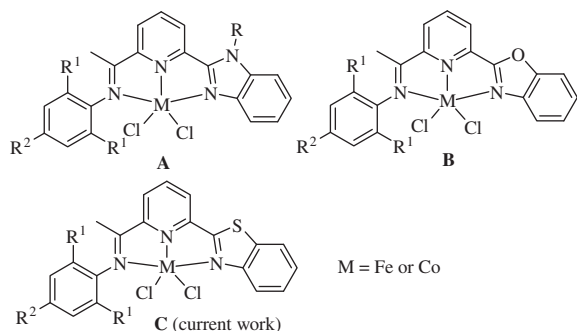
2. Experimental

2.1. General considerations

All manipulations of air- and moisture-sensitive compounds were performed under a nitrogen atmosphere using standard Schlenk techniques. 2-(2-Benzothiazole)-6-acetylpyridine was prepared using a modified procedure according to the literature [34,44]. Toluene was refluxed over sodium-benzophenone and distilled under argon prior to use. Methylaluminoxane (MAO, a 1.46 M solution in toluene) and modified methylaluminoxane (MMAO,

* Corresponding author at: Key Laboratory of Engineering Plastics and Beijing National Laboratory for Molecular Sciences, Institute of Chemistry, Chinese Academy of Sciences, Beijing 100190, China. Tel.: +86 10 62557955; fax: +86 10 62618239.

E-mail address: whsun@iccas.ac.cn (W.-H. Sun).



Scheme 1. Systematic modification of model pro-catalysts.

1.93 M in heptane, 3A) were purchased from Akzo Nobel Corp. Diethylaluminum chloride (Et_2AlCl , 1.7 M in toluene) was purchased from Acros Chemicals. ^1H and ^{13}C NMR spectra were recorded on a Bruker DMX 400 MHz instrument at ambient temperature using TMS as an internal standard. FT-IR spectra were recorded on a Perkin-Elmer System 2000 FT-IR spectrometer. Elemental analyses were carried out using a Flash EA 1112 microanalyzer. GC analyses were performed with a Varian CP-3800 gas chromatograph equipped with a flame ionization detector and a 30 m (0.2 mm i.d., 0.25 μm film thickness) CP-Sil 5 CB column. The yields of oligomers were calculated by referencing with the mass of the solvent, on the basis of the prerequisite that the mass of each fraction was approximately proportional to its integrated areas in the GC trace. Selectivity for the linear α -olefin was defined as (amount of linear α -olefin of all fractions)/(total amount of oligomer products) in percentage. ^1H and ^{13}C NMR spectra of the PE waxes were recorded on a Bruker DMX 300 MHz instrument at 110 $^\circ\text{C}$ in 1,2-dichlorobenzene- d_4 using TMS as the internal standard.

2.2. Synthesis of 2-(benzothiazolyl)-6-iminopyridines

2.2.1. 2,6-Dimethyl-N-(1-(6-(benzothiazol-2-yl)pyridin-2-yl)ethylidene)benzenamine (**L1**)

A solution of 2-(2-benzothiazole)-6-acetylpyridine (1.02 g, 4 mmol), 2,6-dimethylaniline (0.67 g, 4.8 mmol), and a catalytic amount of *p*-toluenesulfonic acid in toluene (50 mL) were refluxed for 12 h. After solvent evaporation, the crude product was purified with petroleum ether/ethyl acetate ($v/v = 15/1$) on an alumina column. The second part to elute was collected and concentrated to give a yellow powder (0.65 g, 45.5 % yield). Mp: 131–132 $^\circ\text{C}$. FT-IR (KBr disk, cm^{-1}): 1641 (m), 1568 (m), 1508 (w), 1436 (w), 1365 (m), 1323 (m), 1204 (m), 1112 (w), 1003 (w), 814 (m), 761 (m). ^1H NMR (400 MHz, CDCl_3 , TMS): δ 8.47 (q, 2H, $J = 7.8$, Py, H_m), 8.11 (d, 1H, $J = 8.1$, Py, H_p), 7.96 (t, 2H, $J = 7.7$, Ar, H), 7.52 (t, 1H, $J = 7.3$, Ar, H), 7.42 (t, 1H, $J = 7.5$, Ar, H), 7.09 (d, 2H, $J = 7.5$, Ar, H), 6.96 (t, 1H, $J = 7.5$, Ar, H), 2.30 (s, 3H, CH_3), 2.33 (s, 3H, CH_3), 2.06 (s, 6H, $2 \times \text{CH}_3$). ^{13}C NMR (300 MHz, CDCl_3 , TMS): δ 169.5, 166.5, 156.0, 154.4, 150.2, 148.6, 137.4, 136.2, 128.2, 127.9, 126.2, 125.6, 125.3, 123.6, 123.1, 122.6, 121.9, 121.5, 117.9, 17.9, 17.6, 16.3. *Anal. Calc.* for $\text{C}_{22}\text{H}_{19}\text{N}_3\text{S}$ (357.47): C, 73.92; H, 5.36; N, 11.75. Found: C, 73.78; H, 5.46; N, 11.66%.

2.2.2. 2,6-Diethyl-N-(1-(6-(benzothiazol-2-yl)pyridin-2-yl)ethylidene)benzenamine (**L2**)

Using the same procedure as for the synthesis of **L1**, **L2** was obtained as a yellow powder in 50.0% yield. Mp: 130–131 $^\circ\text{C}$. FT-IR (KBr disk, cm^{-1}): 1633 (s), 1566 (m), 1454 (s), 1364 (m), 1321 (s), 1235 (m), 1106 (m), 1002 (s), 816 (s), 754 (s). ^1H NMR (300 MHz, CDCl_3 , TMS): δ 8.46 (q, 2H, $J = 7.8$, Py, H_m), 8.11 (m, 1H, $J = 8.1$, Py, H_p), 7.96 (t, 2H, $J = 8.0$, Ar, H), 7.52 (t, 1H, $J = 7.3$, Ar, H), 7.42 (t,

1H, $J = 7.3$, Ar, H), 7.13 (d, 2H, $J = 7.5$, Ar, H), 7.05 (t, 1H, $J = 6.7$, Ar, H), 2.46–2.33 (m, 4H, $2 \times \text{CH}_2$), 2.31 (s, 3H, CH_3), 1.15 (t, 6H, $J = 7.5$, $2 \times \text{CH}_3$). ^{13}C NMR (400 MHz, CDCl_3 , TMS): δ 169.6, 166.3, 156.1, 154.4, 150.3, 147.7, 137.5, 136.3, 131.1, 127.6, 126.3, 126.0, 125.7, 123.7, 123.5, 122.7, 122.0, 121.6, 118.3, 24.7, 24.3, 16.8, 13.8, 13.1. *Anal. Calc.* for $\text{C}_{24}\text{H}_{23}\text{N}_3\text{S}$ (385.52): C, 74.77; H, 6.01; N, 10.90. Found: C, 75.00; H, 5.85; N, 10.75%.

2.2.3. 2,6-Diisopropyl-N-(1-(6-(benzothiazol-2-yl)pyridin-2-yl)ethylidene)benzenamine (**L3**)

Using the same procedure as for the synthesis of **L1**, **L3** was obtained as a yellow powder in 63.6% yield. Mp: 196–197 $^\circ\text{C}$. FT-IR (KBr disk, cm^{-1}): 1653 (s), 1568 (s), 1457 (s), 1366 (m), 1323 (s), 1237 (m), 1111 (s), 1001 (s), 826 (m), 785 (s). ^1H NMR (400 MHz, CDCl_3 , TMS): δ 8.47 (q, 2H, $J = 8.6$, Py, H_m), 8.12 (d, 1H, $J = 8.1$, Py, H_p), 7.99–7.94 (m, 2H, Ar, H), 7.52 (t, 1H, $J = 7.3$, Ar, H), 7.43 (t, 1H, $J = 7.5$, Ar, H), 7.18 (d, 2H, $J = 7.2$, Ar, H), 7.13–7.09 (m, 1H, Ar, H), 2.80–2.73 (m, 2H, $2 \times \text{CH}$), 2.33 (s, 3H, CH_3), 1.18–1.16 (m, 12H, $4 \times \text{CH}_3$). ^{13}C NMR (400 MHz, CDCl_3 , TMS): δ 169.6, 166.3, 156.0, 154.4, 150.2, 146.3, 137.5, 136.2, 135.6, 126.2, 125.6, 123.7, 123.6, 123.0, 122.7, 122.6, 121.9, 121.4, 28.2, 23.2, 22.8, 17.0. *Anal. Calc.* for $\text{C}_{26}\text{H}_{27}\text{N}_3\text{S}$ (413.58): C, 75.51; H, 6.58; N, 10.16. Found: C, 75.87; H, 6.71; N, 10.04%.

2.2.4. 2,4,6-Trimethyl-N-(1-(6-(benzothiazol-2-yl)pyridin-2-yl)ethylidene)benzenamine (**L4**)

Using the same procedure as for the synthesis of **L1**, **L4** was obtained as a yellow powder in 66.0% yield. Mp: 181–182 $^\circ\text{C}$. FT-IR (KBr disk, cm^{-1}): 1648 (s), 1567 (w), 1450 (m), 1363 (m), 1321 (m), 1215 (m), 1111 (w), 1001 (m), 815 (w), 758 (s). ^1H NMR (400 MHz, CDCl_3 , TMS): δ 8.46 (q, 2H, $J = 7.8$, Py, H_m), 8.11 (d, 1H, $J = 8.1$, Py, H_p), 7.96 (t, 2H, $J = 7.7$, Ar, H), 7.52 (t, 1H, $J = 7.2$, Ar, H), 7.43 (t, 1H, $J = 7.1$, Ar, H), 6.91 (s, 2H, Ar, H), 2.31 (s, 3H, CH_3), 2.29 (s, 3H, CH_3), 2.02 (s, 6H, $2 \times \text{CH}_3$). ^{13}C NMR (400 MHz, CDCl_3 , TMS): δ 169.6, 166.7, 156.2, 154.4, 150.2, 146.1, 137.4, 136.2, 132.3, 128.6, 126.2, 125.6, 125.2, 123.6, 122.7, 121.9, 121.5, 20.7, 17.9, 16.3. *Anal. Calc.* for $\text{C}_{23}\text{H}_{21}\text{N}_3\text{S}$ (371.50): C, 74.36; H, 5.70; N, 11.31. Found: C, 74.24; H, 5.42; N, 11.38%.

2.2.5. 2,6-Diethyl-4-methyl-N-(1-(6-(benzothiazol-2-yl)pyridin-2-yl)ethylidene)benzenamine (**L5**)

Using the same procedure as for the synthesis of **L1**, **L5** was obtained as a yellow powder in 60.8 % yield. Mp: 145–146 $^\circ\text{C}$. FT-IR (KBr disk, cm^{-1}): 1638 (s), 1567 (w), 1461 (s), 1364 (m), 1321 (s), 1210 (m), 1112 (w), 1002 (s), 817 (m), 755 (s). ^1H NMR (400 MHz, CDCl_3 , TMS): δ 8.46 (q, 2H, $J = 7.9$, Py), 8.11 (d, 1H, $J = 8.1$, Py), 7.95 (t, 2H, $J = 6.7$, Ar), 7.51 (t, 1H, $J = 7.4$, Ar), 7.41 (t, 1H, $J = 7.6$, Ar), 6.94 (s, 2H, Ar), 2.34 (m, 4H, CH_2), 2.30 (s, 3H, CH_3), 1.14 (t, 6H, $2 \times \text{CH}_3$). ^{13}C NMR (400 MHz, CDCl_3 , TMS): δ 169.8, 166.6, 156.4, 154.6, 150.4, 145.3, 137.7, 136.5, 132.8, 131.2, 126.9, 126.4, 125.8, 123.8, 122.8, 121.1, 121.6, 24.8, 21.2, 16.8, 14.0. *Anal. Calc.* for $\text{C}_{25}\text{H}_{25}\text{N}_3\text{S}$ (399.55): C, 75.15; H, 6.31; N, 10.52. Found: C, 75.27; H, 6.37; N, 10.36%.

2.3. Synthesis of 2-(2-benzothiazolyl)-6-iminopyridyliron dichlorides

2.3.1. 2,6-Dimethyl-N-(1-(6-(benzothiazol-2-yl)pyridin-2-yl)ethylidene)benzenamine FeCl_2 (**Fe1**)

A Shlenk tube was charged with solid 2,6-dimethyl-N-(1-(6-(benzo[d]thiazol-2-yl)pyridin-2-yl)ethylidene)-benzenamine (0.1 g, 0.3 mmol) and $\text{FeCl}_2 \cdot 4\text{H}_2\text{O}$ (0.06 g, 0.3 mmol) and purged three times with argon, followed by the addition of 10 mL ethanol. The reaction mixture was stirred at room temperature for 6 h. The resulting precipitate was filtered off, washed twice with diethyl ether and dried in vacuum to furnish the pure product as a blue powder in 88.0% yield. FT-IR (KBr; cm^{-1}): 1598 (w), 1491 (w),

1430 (w), 1372 (w), 1322 (w), 1256 (m), 1211 (s), 1098 (w), 1050 (w), 807 (m), 774 (s). *Anal. Calc.* for $C_{22}H_{19}Cl_2FeN_3S$ (484.22): C, 54.57; H, 3.95; N, 8.68. Found: C, 54.57; H, 3.82; N, 8.97%. Complexes **Fe2–Fe5** were prepared by the same manner.

2.3.2. 2,6-Diethyl-N-(1-(6-(benzothiazol-2-yl)pyridin-2-yl)ethylidene)benzenamine $FeCl_2$ (**Fe2**)

Yield: 80.2%. FT-IR (KBr disk, cm^{-1}): 1598 (m), 1585 (m), 1491 (w), 1458 (w), 1373 (w), 1320 (w), 1257 (m), 1201 (m), 1085 (w), 812 (m), 768 (s). *Anal. Calc.* for $C_{24}H_{23}Cl_2FeN_3S$ (512.28): C, 56.27; H, 4.53; N, 8.20. Found: C, 56.00; H, 4.55; N, 8.01%.

2.3.3. 2,6-Diisopropyl-N-(1-(6-(benzothiazol-2-yl)pyridin-2-yl)ethylidene)benzenamine $FeCl_2$ (**Fe3**)

Yield: 88.0%. FT-IR (KBr disk, cm^{-1}): 1598 (m), 1568 (w), 1493 (m), 1459 (w), 1427 (w), 1371 (m), 1319 (w), 1257 (m), 1199 (m), 1100 (w), 1018 (w), 816 (w), 761 (m). *Anal. Calc.* for $C_{26}H_{27}Cl_2FeN_3S$ (540.33): C, 57.79; H, 5.04; N, 7.78. Found: C, 57.53; H, 5.15; N, 7.64%.

2.3.4. 2,4,6-Trimethyl-N-(1-(6-(benzothiazol-2-yl)pyridin-2-yl)ethylidene)benzenamine $FeCl_2$ (**Fe4**)

Yield: 76.7%. FT-IR (KBr disk, cm^{-1}): 1599 (m), 1560 (w), 1492 (w), 1457 (w), 1428 (w), 1373 (w), 1324 (w), 1252 (m), 1218 (m), 1187 (w), 1086 (w), 1018 (w), 803 (w), 779 (m). *Anal. Calc.* for $C_{23}H_{21}Cl_2FeN_3S$ (498.25): C, 55.44; H, 4.25; N, 8.43. Found: C, 55.26; H, 4.37; N, 8.28%.

2.3.5. 2,6-Diethyl-4-methyl-N-(1-(6-(benzothiazol-2-yl)pyridin-2-yl)ethylidene)benzenamine $FeCl_2$ (**Fe5**)

Yield: 80.0%. FT-IR (KBr disk, cm^{-1}): 1598 (m), 1560 (w), 1493 (s), 1459 (s), 1429 (m), 1372 (m), 1323 (m), 1258 (s), 1213 (s), 1188 (m), 1018 (w), 803 (w), 779 (m). *Anal. Calc.* for $C_{25}H_{25}Cl_2FeN_3S$ (526.30): C, 57.05; H, 4.79; N, 7.98. Found: C, 56.66; H, 4.82; N, 7.96%.

2.4. Synthesis of 2-(2-benzothiazolyl)-6-iminopyridylcobalt dichlorides

2.4.1. 2,6-Dimethyl-N-(1-(6-(benzothiazol-2-yl)pyridin-2-yl)ethylidene)benzenamine $CoCl_2$ (**Co1**)

All the cobalt complexes were prepared in good yield with the same synthetic procedure: An ethanol solution of equivalent amount of $CoCl_2$ was added to the ethanol solution of the corresponding ligand, and the mixture was stirred for 6 h at room temperature. The resultant precipitate was collected, washed with diethyl ether and dried in vacuum. **Co1** obtained as green powder in 88.0% yield. FT-IR (KBr; cm^{-1}): 1599 (m), 1570 (w), 1492 (m), 1468 (w), 1429 (w), 1372 (m), 1323 (w), 1254 (s), 1212 (s), 1097 (w), 1025 (w), 808 (w), 775 (s). *Anal. Calc.* for $C_{22}H_{19}Cl_2CoN_3S$ (487.31): C, 54.22; H, 3.93; N, 8.62. Found: C, 54.13; H, 4.18; N, 8.54%.

2.4.2. 2,6-Diethyl-N-(1-(6-(benzothiazol-2-yl)pyridin-2-yl)ethylidene)benzenamine $CoCl_2$ (**Co2**)

Yield: 80.2%. FT-IR (KBr disk, cm^{-1}): 1599 (m), 1585 (s), 1491 (s), 1459 (w), 1373 (m), 1321 (w), 1256 (s), 1202 (s), 1024 (w), 814 (m), 767 (s). *Anal. Calc.* for $C_{24}H_{23}Cl_2CoN_3S$ (515.36): C, 55.93; H, 4.50; N, 8.15. Found: C, 55.57; H, 4.54; N, 8.06%.

2.4.3. 2,6-Diisopropyl-N-(1-(6-(benzothiazol-2-yl)pyridin-2-yl)ethylidene)benzenamine $CoCl_2$ (**Co3**)

Yield: 76.0%. FT-IR (KBr disk, cm^{-1}): 1599 (m), 1569 (w), 1493 (m), 1459 (w), 1426 (w), 1371 (m), 1317 (w), 1258 (m), 1199 (m), 1096 (w), 1024 (w), 817 (w), 770 (m). *Anal. Calc.* for

$C_{26}H_{27}Cl_2CoN_3S$ (543.42): C, 57.47; H, 5.01; N, 7.73. Found: C, 57.28; H, 5.11; N, 7.66%.

2.4.4. 2,4,6-Trimethyl-N-(1-(6-(benzothiazol-2-yl)pyridin-2-yl)ethylidene)benzenamine $CoCl_2$ (**Co4**)

Yield: 82.4%. FT-IR (KBr disk, cm^{-1}): 1599 (m), 1568 (w), 1492 (s), 1459 (w), 1428 (w), 1372 (w), 1324 (w), 1251 (m), 1218 (m), 1187 (m), 1022 (w), 804 (w), 779 (m). *Anal. Calc.* for $C_{23}H_{21}Cl_2CoN_3S$ (501.34): C, 55.10; H, 4.22; N, 8.38. Found: C, 55.00; H, 4.30; N, 8.30%.

2.4.5. 2,6-Diethyl-4-methyl-N-(1-(6-(benzothiazol-2-yl)pyridin-2-yl)ethylidene)benzenamine $CoCl_2$ (**Co5**)

Yield: 82.0%. FT-IR (KBr disk, cm^{-1}): 1597 (m), 1568 (w), 1487 (s), 1459 (s), 1425 (w), 1371 (m), 1321 (m), 1256 (s), 1213 (m), 1184 (w), 1023 (w), 813 (m), 774 (m). *Anal. Calc.* for $C_{25}H_{25}Cl_2CoN_3S$ (529.39): C, 56.72; H, 4.76; N, 7.94. Found: C, 56.59; H, 4.79; N, 7.97%.

2.5. General procedure for ethylene reactivation

Ethylene oligomerizations and polymerizations were performed in a 500 mL stainless steel autoclave equipped with a mechanical stirrer and a temperature controller. Toluene, the desired amount of modified methylaluminoxane, and a toluene solution of the catalyst precursor was added to the reactor in this order under an ethylene atmosphere, the total volume was 100 mL. When the desired reaction temperature was reached, ethylene at 10 atm pressure was introduced to start the reaction, and the ethylene pressure was maintained by a constant feed of ethylene during reaction period. After that, the reaction was stopped, and the autoclave was cooled in an ice-water bath. Then the pressure was released and a small amount of the reaction solution was collected, which was then quenched with HCl-acidified ethanol (5%). The organic layer was analyzed as quickly as possible by gas chromatography (GC) to determine the composition and mass distribution according to GC–Mass spectrum of oligomers. Then the remaining reaction mixture was quenched with HCl-acidified ethanol (5%) in order to collect polyethylene obtained with being additionally washed with ethanol, and dried under vacuum at 60 °C to constant weight.

2.6. X-ray crystallography

Single-crystals of **Fe2**, **Fe3** and **Co3** suitable for X-ray diffraction were obtained by the slow diffusion of diethyl ether into the methanol solution. Data were collected on a Rigaku RAXIS Rapid IP diffractometer with graphite monochromated Mo $K\alpha$ radiation ($\lambda = 0.71073 \text{ \AA}$). Cell parameters were obtained by global refinement of the positions of all collected reflections. Intensities were corrected for Lorentz and polarization effects and empirical absorption. The structures were solved by direct methods and refined by full-matrix least squares on F^2 . All hydrogen atoms were placed in calculated positions. Structure solution and refinement were performed by using the SHELXL-97 package [45]. Crystal data and processing parameters for **Fe2**, **Fe3** and **Co3** are summarized in Table 1.

3. Results and discussion

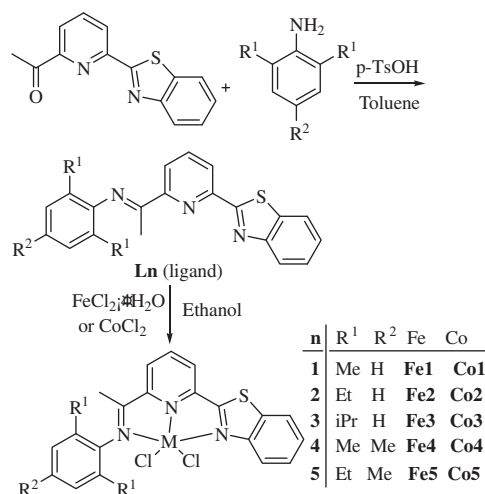
3.1. 2-(2-Benzothiazolyl)-6-(1-(arylimino)ethyl)pyridines and their iron and cobalt complexes

The 2-(2-benzothiazolyl)-6-acetylpyridine was prepared according to our procedure [31–35], and then reacted with anilines to form 2-(2-benzothiazolyl)-6-(1-aryliminoethyl)pyridines

Table 1
Crystal data and structure refinement details for **Fe2**, **Fe3** and **Co3**.

	Fe2	Fe3	Co3
Empirical formula	C ₂₄ H ₂₃ Cl ₂ FeN ₃ S	C ₂₆ H ₂₇ Cl ₂ FeN ₃ S	C ₂₆ H ₂₇ Cl ₂ CoN ₃ S
Formula weight	512.26	540.32	543.40
T (K)	293(2)	173(2)	173(2)
Wavelength (Å)	0.71073	0.71073	0.71073
Crystal system	monoclinic	monoclinic	monoclinic
Space group	<i>P2₁/c</i>	<i>P2₁/c</i>	<i>P2₁/c</i>
<i>a</i> (Å)	9.225 (1)	9.374 (1)	9.320 (1)
<i>b</i> (Å)	14.652(3)	14.918(3)	14.950(3)
<i>c</i> (Å)	18.154(4)	18.285(4)	18.323(4)
β (°)	96.75(3)	93.20(3)	92.79(3)
<i>V</i> (Å ³)	2436.9(8)	2553.0(9)	2550.2(9)
<i>Z</i>	4	4	4
<i>D</i> _{calc} (Mg m ⁻³)	1.396	1.406	1.415
μ (mm ⁻¹)	0.940	0.901	0.984
<i>F</i> (0 0 0)	1056	1120	1124
Crystal size (mm)	0.39 × 0.39 × 0.34	0.13 × 0.13 × 0.12	0.20 × 0.20 × 0.20
θ Range (°)	2.62–25.00	1.76–25.00	2.58–25.00
Limiting indices	–10 ≤ <i>h</i> ≤ 10 –17 ≤ <i>k</i> ≤ 17 –21 ≤ <i>l</i> ≤ 21	–11 ≤ <i>h</i> ≤ 10 –17 ≤ <i>k</i> ≤ 17 –21 ≤ <i>l</i> ≤ 16	–11 ≤ <i>h</i> ≤ 10 –16 ≤ <i>k</i> ≤ 17 –21 ≤ <i>l</i> ≤ 21
Number of reflections collected	8205	15 716	16 923
Number of unique reflections	4274	4473	4474
Completeness to θ (%)	99.7 ($\theta = 25.00^\circ$)	99.7 ($\theta = 25.00^\circ$)	99.8 ($\theta = 25.00^\circ$)
Abs. Cor.	multi-scan	multi-scan	multi-scan
Number of parameters	290	298	298
Goodness of fit on <i>F</i> ²	1.197	1.152	1.162
Final <i>R</i> indices (<i>I</i> > 2 σ (<i>I</i>))	<i>R</i> ₁ = 0.0664 <i>wR</i> ₂ = 0.1264	<i>R</i> ₁ = 0.0505 <i>wR</i> ₂ = 0.1005	<i>R</i> ₁ = 0.0464 <i>wR</i> ₂ = 0.1103
<i>R</i> indices (all data)	<i>R</i> ₁ = 0.0923 <i>wR</i> ₂ = 0.1362	<i>R</i> ₁ = 0.0573 <i>wR</i> ₂ = 0.1040	<i>R</i> ₁ = 0.0514 <i>wR</i> ₂ = 0.1134
Largest difference in peak and hole (e Å ⁻³)	0.463, –0.298	0.531, –0.425	0.473, –0.401

(**L**, Scheme 2). The blue iron(II) complexes **Fe1–Fe5** were prepared in good yields by stirring stoichiometric amounts of FeCl₂ and the corresponding ligand in ethanol for 6 h at room temperature (Scheme 2). All ferrous complexes were characterized by FT-IR spectra and elemental analyses, and agreed with the formula LFeCl₂. While the C=N stretching frequencies of the free ligands appear in the range of 1633–1653 cm⁻¹, the C=N stretching vibrations were shifted to lower frequencies of 1598–1599 cm⁻¹ in complexes **Fe1–Fe5**. This shift and the reduced peaks' intensities indicate an effective coordination of iron by the imino nitrogen. By the same procedure, the green cobalt complexes **Co1–Co5** were conveniently prepared in good yields (Scheme 2). These cobalt complexes are stable in both solution and solid state. In addition, the molecular structures of the complexes **Fe2**, **Fe3** and **Co3** were determined by single crystal X-ray diffraction.



Scheme 2. Synthesis of the iron and cobalt complexes.

3.2. Crystal structures

Single crystals of **Fe2**, **Fe3** and **Co3** suitable for single-crystal X-ray diffraction were grown from their methanol solutions layered with diethyl ether. In complex **Fe2** (Fig. 1), the coordination geometry around iron is a distorted trigonal-bipyramidal, in which the pyridine-nitrogen N(1) and two chlorine atoms approximately lie in an equatorial plane with the deviation from the plane of 0.0598 Å for iron atom. The equatorial plane and the trans-nitrogen atoms N(2) and N(3) form the angle of 88.9°. Similar to the iron analogs bearing 2-(2-benzimidazolyl)-6-acetylpyridines [31–33], the 2,6-dimethylphenyl is oriented nearly orthogonally (83.4°) to the coordination plane (N(3)–N(1)–N(2)).

The similar coordination geometry also occurs within complex **Fe3** (Fig. 2). The fused-rings of Fe(1)–N(2)–C(6)–C(7)–N(1)–Fe(1) and Fe(1)–N(1)–C(11)–C(12)–N(3)–Fe(1) are co-planar and nearly perpendicular to the aryl ring linked through the imino-group

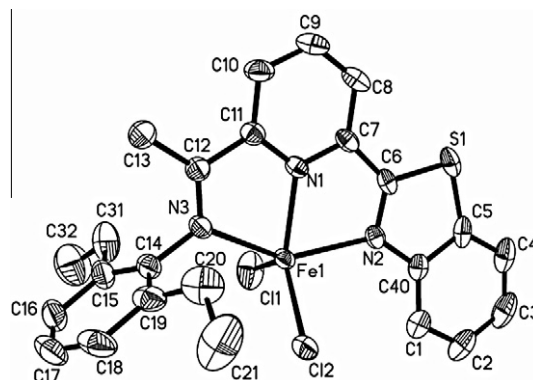


Fig. 1. Molecular structure of **Fe2** with thermal ellipsoids at the 30% probability level. Hydrogen atoms have been omitted for clarity.

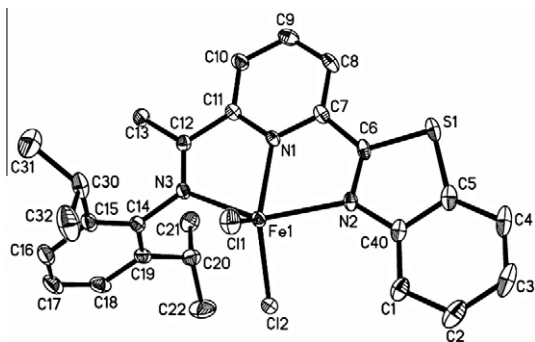


Fig. 2. Molecular structure of **Fe3** with thermal ellipsoids at the 30% probability level. Hydrogen atoms have been omitted for clarity.

(84.1°), whereas the dihedral angle between the aryl plane linked on imino-group and the pyridyl group is 82.8°. The Fe–N bond lengths follow the order Fe(1)–N(3) > Fe(1)–N(2) > Fe(1)–N(1) while the two Fe–Cl bond lengths are almost equal. This is a significant difference compared to the distorted square-pyramidal coordination observed in the iron complexes ligated by 2-benzimidazolyl-6-iminopyridines [31–33] or 2-benzoxazolyl-6-iminopyridines [34,35]. The N(2)–C(6) bond distance is 1.312(4) Å displaying clear C=N double bond character, shorter than C(6)–O(1) by 1.722(3) Å.

The coordination geometry of complex **Co3** (Fig. 3) is best described as a distorted trigonal-bipyramidal with the equatorial plane defined by the N(1), Cl(1) and Cl(2), and the position of the cobalt atom deviates 0.0215 Å from the equatorial plane. Three nitrogen atoms (N(1), N(2) and N(3)) occupy axial plane. The dihedral angle between axial and equatorial planes with cobalt center forms 148.3°. This is consistent with observations of its cobalt analogs [31–33,35]. Due to the asymmetry of the molecule, the Co–N bonds are significantly different, Co(1)–N(2) = 2.234(2) Å and Co(1)–N(3) = 2.267(2) Å; while the C–N_{imino} bonds, (N(2)–C(6) = 1.313(4) Å and N(3)–C(12) = 1.287(4) Å, are typical and within the standard deviation [22–26,28–35,46–50].

3.3. Ethylene oligomerization and polymerization

3.3.1. Ethylene reactivity by iron complexes

Various alkylaluminiums such as methylaluminumoxane (MAO), modified methylaluminumoxane (MMAO) and diethylaluminum chloride (Et₂AlCl) were used in evaluating the ethylene activation by **Fe1**. Since low activity was observed at ambient ethylene

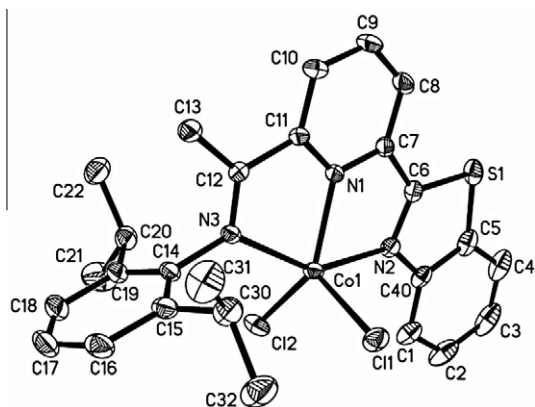


Fig. 3. Molecular structure of **Co3** with thermal ellipsoids at the 30% probability level. Hydrogen atoms have been omitted for clarity.

pressure, the investigation was performed at 10 atm C₂H₄ (Table 2). The highest activity was obtained with MMAO. The performance with regard to both catalytic activity and α -olefins' selectivity is better than for its analog bearing 2-(benzimidazolyl)-6-aminopyridines [31–33].

The influence of reaction parameters such as the molar ratio of Al/Fe and reaction temperature was investigated in detail (Table 3). Notably increasing the molar ratio from 300 to 750, the activities were dramatically increased (entries 1–3 in Table 3), which might be attributed to the scavenging of any impurities. A further increase of the molar ratio to 1000 (entry 4 in Table 3) decreased the activity. The distributions of oligomers semi-resembled the Schulz–Flory rule [51,52], in which the probability of chain propagation is given by K , where $K = (\text{rate of propagation}) / ((\text{rate of propagation}) + (\text{rate of chain transfer})) = (\text{moles of } C_{14}) / (\text{moles of } C_{12})$. The Al/Fe molar ratio had little influence on the oligomer distribution and K values. Employing the optimum Al/Fe ratio of 750, elevating the reaction temperature from 30 °C to 60 °C resulted in a great decrease in productivity (entries 3 and 5–7 in Table 3). This probably caused with the thermally unstable active species and lower ethylene absorption in solution at higher temperature [5,53]. The oligomers' distribution became narrower with more shorter chain olefins, which attribute to faster β -hydrogen elimination at higher temperature.

In the **Fe1**/MMAO system, the ethylene reactivity was steadily maintained over forty minutes (entries 1–4 in Table 4). Prolonging the reaction time to one hour, however, resulted in decreased activities for both ethylene oligomerization and polymerization (entries 5 and 6 in Table 4). Regarding to polyethylene waxes obtained, vinyl-nature of long-chain α -olefin was confirmed by the ¹H and ¹³C NMR spectra.

Subsequently, all iron pro-catalysts were investigated under the optimum condition, and the results were tabulated in Table 5. Regarding complexes **Fe1–Fe3** containing 2,6-dialkyl substituents (entries 1–3 in Table 5), bulkier R¹ groups cause lower activities in both oligomerization and polymerization. We believe that the bulkier substituents hinder the approach of ethylene to the active species. Such tendency was similar with the observation by the iron analogs bearing 2-(1-isopropyl-2-benzimidazolyl)-6-aminopyridines [32], but different to those by iron analogs having 2-(1*H*-2-benzimidazolyl)-6-aminopyridines [33] and 2-(1-methyl-2-benzimidazolyl)-6-iminopyridines [31]. Regarding to the oligomer distribution, the bulkier R¹ substituents increase the content of C₄. In addition, the *para*-methyl of the aryl ring positively affected the activity of iron pro-catalyst (entries 4 and 5 in Table 5) due to better solubility caused. Such phenomenon was also observed by iron pro-catalysts ligated by 2-quinoxalanyl-6-iminopyridines [30] and 2-(1-isopropyl-2-benzimidazolyl)-6-iminopyridines [32]. The activities of the current iron pro-catalysts are comparable to those of common bis(imino)pyridyliron pro-catalysts [2–4], but the current iron catalytic systems show higher selectivity of α -olefins in ethylene oligomerization.

3.3.2. Ethylene oligomerization by cobalt complexes

Using complex **Co1** to select the co-catalyst (entries 1–3 in Table 6), MMAO was found to be the most suitable one. Within molar ratios of MMAO/Co from 200 to 1000 (entries 2 and 4–6 in Table 6), the best activity of ethylene oligomerization was observed at 500. At the MMAO/Co ratio of 500, further elevation of the reaction temperature lowered activity (entries 5, 7 and 8 in Table 6). As with their iron analogs [5,53], the cobalt active species are thermally unstable, moreover, with a lower solubility of ethylene at higher temperature. The cobalt complexes were investigated in detail with the MMAO/Co molar ratio of 500 at room temperature (Table 6).

Table 2
Selection of a suitable cocatalyst based on **Fe1**.^a

Entry	Cocat.	Al/Fe	Oligomer activity ^b	Oligomer distribution ^c	Polymer activity ^b
1	MAO	1000	14.4	C ₄ –C ₂₈	3.43
2	MMAO	1000	59.3	C ₄ –C ₂₈	6.06
3	Et ₂ AlCl	200	4.2	C ₄ –C ₈	trace

^a Conditions: 5 μmol **Fe1**; 10 atm ethylene; 30 min, 30 °C; 100 mL toluene.^b 10³ g mol⁻¹(Fe) h⁻¹.^c Determined by GC; ΣC denotes the total amount of oligomers.**Table 3**
Ethylene oligomerization and polymerization by **Fe1**/MMAO.^a

Entry	Al/Fe	T (°C)	K	α-O ^b (%)	Activity ^c		Oligomer distribn (%) ^d			
					Oligomer	Wax	C ₄ /ΣC	C ₆ /ΣC	C ₈ /ΣC	ΣC _{≥10} /ΣC
1	300	30	0.37	94.4	49.3	3.66	64.1	23.5	8.0	4.4
2	500	30	0.42	97.3	66.2	7.01	62.4	23.8	8.4	5.4
3	750	30	0.43	97.8	93.5	6.15	61.0	24.3	8.2	6.5
4	1000	30	0.42	97.5	59.3	6.06	62.6	24.3	7.8	5.3
5	750	40	0.43	97.6	57.5	3.84	64.5	21.8	7.0	6.7
6	750	50	0.42	97.5	44.6	3.17	65.1	21.9	6.8	6.2
7	750	60	0.40	99.9	1.2	0.85	66.8	20.2	7.0	6.0

^a Conditions: 5 μmol **Fe1**; 10 atm ethylene; 30 min, 100 mL toluene.^b α-Olefin percentage determined by GC.^c 10³ g mol⁻¹(Fe) h⁻¹.^d Determined by GC; ΣC denotes the total amount of oligomers.**Table 4**
Polymerization and oligomerization of ethylene with **Fe1**/MMAO.^a

Entry	t (min)	K	α-O ^b (%)	Activity ^c		Oligomer distribution (%) ^d			
				Oligomer	Wax	C ₄ /ΣC	C ₆ /ΣC	C ₈ /ΣC	ΣC _{≥10} /ΣC
1	10	0.42	99.7	81.3	5.15	64.7	23.8	7.2	4.3
2	20	0.41	97.4	102	6.14	62.8	25.0	7.5	4.7
3	30	0.43	97.8	93.5	6.15	61.0	24.3	8.2	6.5
4	40	0.40	97.9	84.2	5.09	61.9	25.3	7.6	5.2
5	50	0.39	97.1	68.4	4.11	61.8	25.6	7.4	5.2
6	60	0.40	93.1	57.6	3.49	61.4	24.7	8.0	5.9

^a Conditions: 5 μmol **Fe1**; 10 atm ethylene; 750 equiv. MMAO; 30 °C; 100 mL toluene.^b α-Olefin percentage determined by GC.^c 10³ g mol⁻¹(Fe) h⁻¹.^d Determined by GC; ΣC denotes the total amount of oligomers.**Table 5**
Polymerization and oligomerization of ethylene with **Fe1–Fe5**/MMAO.^a

Entry	Cat.	α-O ^b (%)	Activity ^c		Oligomer distribution (%) ^d			
			Oligomer	Wax	C ₄ /ΣC	C ₆ /ΣC	C ₈ /ΣC	ΣC _{≥10} /ΣC
1	Fe1	97.8	93.5	6.15	61.0	24.3	8.2	6.5
2	Fe2	97.5	77.9	1.25	72.4	20.5	5.2	1.9
3	Fe3	99.2	49.3	0.28	87.9	10.0	2.0	0.1
4	Fe4	96.6	110	4.91	63.0	24.8	7.7	4.5
5	Fe5	97.4	81.8	1.12	68.3	20.3	6.0	5.4

^a Conditions: 5 μmol Fe; 750 equiv. MMAO; 10 atm ethylene; 30 °C; 30 min; 100 mL toluene.^b α-Olefin percentage determined by GC.^c 10³ g mol⁻¹(Fe) h⁻¹.^d Determined by GC; ΣC denotes the total amount of oligomers.

Their catalytic activities were significantly affected by the ligands' environment, and their activity varied in the order **Co3** > **Co2** > **Co1** and **Co5** > **Co4** > **Co2** > **Co1**. The bulkier the substituents were, the higher activity cobalt pro-catalysts performed; this is naturally different to their iron analogs. It was believed that bulkier substituents might be helpful for both the solubility of complexes and stability of active species due to less exposing to impurity reactants. Such observation is different to their cobalt analogs ligated by 2-benzimidazolyl-6-iminopyridines [31,32]

and 2-benzoxazolyl-6-(1-(arylimino)ethyl)pyridine [34,35]. The introducing one *para*-methyl resulted in higher activity (entries 11, 12 in Table 5) due to better solubility. In general, cobalt pro-catalysts showed much lower activities than their iron analogs. Such phenomena have commonly been observed within previous pro-catalysts.

Compared with their analogs bearing 2-benzimidazole-6-(1-aryliminoethyl)pyridines [31–33], 2-benzoxazolyl-6-(1-(arylimino)ethyl)pyridine [35], and 2,6-bis(2-oxazolin-2-yl)pyridine [54],

Table 6
Oligomerization of ethylene with cobalt pro-catalysts.^a

Entry	Cat.	Cocat.	Al/Co	T (°C)	Activity ^b	Oligomer distribution (%) ^c		
						C ₄ /ΣC	C ₆ /ΣC	α-C ₄
1	Co1	MAO	1000	20	1.48	100	0	94.2
2	Co1	MMAO	1000	20	3.00	98.6	1.4	100
3	Co1	Et ₂ AlCl	200	20	trace	–	–	–
4	Co1	MMAO	200	20	4.01	100	0	100
5	Co1	MMAO	500	20	7.94	98.1	1.9	100
6	Co1	MMAO	750	20	3.54	98.0	2.0	100
7	Co1	MMAO	500	40	4.50	99.6	0.4	96.6
8	Co1	MMAO	500	50	0.90	98.8	1.2	100
9	Co2	MMAO	500	20	8.85	98.3	1.7	100
10	Co3	MMAO	500	20	15.80	98.7	1.3	100
11	Co4	MMAO	500	20	9.90	97.0	3.0	100
12	Co5	MMAO	500	20	9.98	100	0	100

^a Conditions: 5 μmol Co; 10 atm ethylene; 30 min, 100 mL toluene.^b 10⁵ g mol⁻¹(Co) h⁻¹.^c Determined by GC; ΣC denotes the total amount of oligomers.

the current cobalt pro-catalysts showed higher production activity towards ethylene oligomerization and polymerization. However, the cobalt pro-catalysts did not perform ethylene polymerization at the elevated reaction temperature, which were observed by 2-benzoxazolyl-6-iminopyridylcobalt pro-catalysts [35]. These results by cobalt pro-catalysts resembled the simulation conclusion on the correlation between the activity and net charge of late-transition metal complexes, in which the stronger the electron-donating ability of the ligand, the lower is the net charge on the metal, resulted a lower activity [38,55].

4. Conclusion

The iron and cobalt complexes bearing 2-(benzothiazolyl)-6-(1-(arylimino)ethyl)pyridines provide accessible pro-catalysts for ethylene oligomerization. Though the reaction at elevated temperature would result in a deactivation and a lower selectivity for α-olefins, the iron pro-catalysts show activities of up to 10⁷ g mol⁻¹(Fe) h⁻¹ for oligomers and 7.01 × 10⁵ g mol⁻¹(Fe) h⁻¹ for waxes in the presence of MMAO. In most cases, the waxes obtained have been confirmed to be vinyl-type olefins. The cobalt pro-catalysts show moderate activity.

Acknowledgments

This work is supported by NSFC No. 20874105 and MOST 863 program No. 2009AA033601. The authors are grateful to Rainer Glaser (Department of Chemistry, University of Missouri-Columbia, Columbia, MO) for proofreading the English language.

Appendix A. Supplementary material

CCDC 793698, 793699 and 793700 contain the supplementary crystallographic data for complexes **Fe2**, **Fe3** and **Co3**, respectively. These data can be obtained free of charge from The Cambridge Crystallographic Data Centre via www.ccdc.cam.ac.uk/data_request/cif. Supplementary data associated with this article can be found, in the online version, at [doi:10.1016/j.ica.2011.06.037](https://doi.org/10.1016/j.ica.2011.06.037).

References

- [1] A.M.A. Bennett (Dupont), PCT Int. Appl., WO9827124 Al, 1998.
- [2] B.L. Small, M. Brookhart, A.M.A. Bennett, J. Am. Chem. Soc. 120 (1998) 4049.
- [3] G.J.P. Britovsek, V.C. Gibson, B.S. Kimberley, P.J. Maddox, S.J. McTavish, G.A. Solan, A.J.P. White, D.J. Williams, Chem. Commun. (1998) 849.
- [4] B.L. Small, M. Brookhart, J. Am. Chem. Soc. 120 (1998) 7143.
- [5] G.J.P. Britovsek, M. Bruce, V.C. Gibson, B.S. Kimberley, P.J. Maddox, S. Mastroianni, S.J. McTavish, C. Redshaw, G.A. Solan, S. Strömberg, A.J.P. White, D.J. Williams, J. Am. Chem. Soc. 121 (1999) 8728.
- [6] Y. Chen, C. Qian, J. Sun, Organometallics 22 (2003) 1231.
- [7] Z. Ma, W.-H. Sun, Z. Li, C. Shao, Y. Hu, X. Li, Polym. Int. 51 (2002) 994.
- [8] B.L. Small, R. Rios, E.R. Fernandez, M.J. Carney, Organometallics 26 (2007) 1744.
- [9] L. Guo, H. Gao, L. Zhang, F. Zhu, Q. Wu, Organometallics 29 (2010) 2118.
- [10] J. Yu, L. Hao, W. Zhang, X. Hao, W.-H. Sun, Chem. Commun. 47 (2011) 3257.
- [11] F. Pelascini, M. Wesolek, F. Peruch, P.J. Lutz, Eur. J. Inorg. Chem. (2006) 4309.
- [12] J. Cámpora, A.M. Naz, P. Palma, E. Álvarez, M.L. Reyes, Organometallics 24 (2005) 4878.
- [13] B. Bianchini, G. Mantovani, A. Meli, F. Migliacci, F. Zanobini, F. Laschi, A. Sommazzi, Eur. J. Inorg. Chem. (2003) 1620.
- [14] B.L. Small, Organometallics 22 (2003) 3178.
- [15] B.L. Small, M.J. Carney, D.M. Holman, C.E. O'Rourke, J.A. Halfen, Macromolecules 37 (2004) 4375.
- [16] C. Bianchini, D. Gatteschi, G. Giambastiani, I.G. Rios, A. Ienco, F. Laschi, C. Mealli, A. Meli, L. Sorace, A. Toti, F. Vizza, Organometallics 26 (2007) 726.
- [17] P. Barbaro, C. Bianchini, G. Giambastiani, I.G. Rios, A. Meli, W. Oberhauser, A.M. Segarra, L. Sorace, A. Toti, Organometallics 26 (2007) 4639.
- [18] C. Wallenhorst, G. Kehr, H. Luftmann, R. Fröhlich, G. Erker, Organometallics 27 (2008) 6547.
- [19] W.-H. Sun, X. Tang, T. Gao, B. Wu, W. Zhang, H. Ma, Organometallics 23 (2004) 5037.
- [20] C. Bianchini, G. Mantovani, A. Meli, F. Migliacci, Organometallics 22 (2003) 2545.
- [21] C. Bianchini, G. Giambastiani, G. Mantovani, A. Meli, D. Mimeo, J. Organomet. Chem. 689 (2004) 1356.
- [22] W.-H. Sun, S. Jie, S. Zhang, W. Zhang, Y. Song, H. Ma, J. Chen, K. Wedeking, R. Fröhlich, Organometallics 25 (2006) 666.
- [23] S. Jie, S. Zhang, K. Wedeking, W. Zhang, H. Ma, X. Lu, Y. Deng, W.-H. Sun, C.R. Chim. 9 (2006) 1500.
- [24] S. Jie, S. Zhang, W.-H. Sun, X. Kuang, T. Liu, J. Guo, J. Mol. Catal. A Chem. 269 (2007) 85.
- [25] S. Jie, S. Zhang, W.-H. Sun, Eur. J. Inorg. Chem. 35 (2007) 5584.
- [26] M. Zhang, W. Zhang, T. Xiao, J.-F. Xiang, X. Hao, W.-H. Sun, J. Mol. Catal. A Chem. 320 (2010) 92.
- [27] M. Zhang, R. Gao, X. Hao, W.-H. Sun, J. Organomet. Chem. 693 (2008) 3867.
- [28] M. Zhang, P. Hao, W. Zuo, S. Jie, W.-H. Sun, J. Organomet. Chem. 693 (2008) 483.
- [29] K. Wang, K. Wedeking, W. Zuo, D. Zhang, W.-H. Sun, J. Organomet. Chem. 693 (2008) 1073.
- [30] W.-H. Sun, P. Hao, G. Li, S. Zhang, W. Wang, J. Yi, M. Asma, N. Tang, J. Organomet. Chem. 692 (2007) 4506.
- [31] W.-H. Sun, P. Hao, S. Zhang, Q. Shi, W. Zuo, X. Tang, Organometallics 26 (2007) 2720.
- [32] Y. Chen, P. Hao, W. Zuo, K. Gao, W.-H. Sun, J. Organomet. Chem. 693 (2008) 1829.
- [33] L. Xiao, R. Gao, M. Zhang, Y. Li, X. Cao, W.-H. Sun, Organometallics 28 (2009) 2225.
- [34] R. Gao, Y. Li, F. Wang, W.-H. Sun, M. Bochmann, Eur. J. Inorg. Chem. 27 (2009) 4149.
- [35] R. Gao, K. Wang, Y. Li, F. Wang, W.-H. Sun, C. Redshaw, M. Bochmann, J. Mol. Catal. A Chem. 309 (2009) 166.
- [36] S.D. Ittel, L.K. Johnson, M. Brookhart, Chem. Rev. 100 (2000) 1169.
- [37] V.C. Gibson, S.K. Spitzmesser, Chem. Rev. 103 (2003) 283.
- [38] C. Bianchini, G. Giambastiani, I.G. Rios, G. Mantovani, A. Meli, A.M. Segarra, Coord. Chem. Rev. 250 (2006) 1391.
- [39] V.C. Gibson, C. Redshaw, G.A. Solan, Chem. Rev. 107 (2007) 1745.
- [40] W.-H. Sun, S. Zhang, W. Zuo, C.R. Chim. 11 (2008) 307.

- [41] C. Bianchini, G. Giambastiani, L. Luconi, A. Meli, *Coord. Chem. Rev.* 254 (2010) 431.
- [42] S. Jie, W.-H. Sun, T. Xiao, *Chin. J. Polym. Sci.* 28 (2010) 299.
- [43] M. Zhang, K. Wang, W.-H. Sun, *Dalton Trans.* (2009) 6354.
- [44] R. Gao, M. Zhang, T. Liang, F. Wang, W.-H. Sun, *Organometallics* 27 (2008) 5641.
- [45] G.M. Sheldrick, *SHELXTL-97 Program for the Refinement of Crystal Structures*, University of Göttingen, Germany, 1997.
- [46] J. Càmpera, A.M. Naz, P. Palma, A. Rodríguez-Delgado, E. Álvarez, I. Tritto, L. Boggioni, *Eur. J. Inorg. Chem.* (2008) 1871.
- [47] A.P. Armitage, Y.D.M. Champouret, H. Grigoli, J.D.A. Pelletier, K. Singh, G.A. Solan, *Eur. J. Inorg. Chem.* (2008) 4597.
- [48] A.S. Ionkin, W.J. Marshall, D.J. Adelman, B.B. Fones, B.M. Fish, M.F. Schifffhauer, *Organometallics* 27 (2008) 1147.
- [49] A.S. Ionkin, W.J. Marshall, D.J. Adelman, B.B. Fones, B.M. Fish, M.F. Schifffhauer, *Organometallics* 27 (2008) 1902.
- [50] J. Volbeda, A. Meetsma, M.W. Bouwkamp, *Organometallics* 28 (2009) 209.
- [51] G.V.Z. Schulz, *Phys. Chem., Abt. B* 43 (1939) 25.
- [52] P.J. Flory, *J. Am. Chem. Soc.* 62 (1940) 1561.
- [53] G.J.P. Britovsek, S. Mastroianni, G.A. Solan, S.P.D. Baugh, C. Redshaw, V.C. Gibson, A.J.P. White, D.J. Williams, M.R.J. Elsegood, *Chem. Eur. J.* 6 (2000) 2221.
- [54] K. Nomura, S. Warit, Y. Imanishi, *Bull. Chem. Soc. Jpn.* 73 (2000) 599.
- [55] T. Zhang, W.-H. Sun, T. Li, X. Yang, *J. Mol. Catal. A Chem.* 218 (2004) 119.